Determining the possible lattice sites of two unknown defects in orthoclase from the polarization effects in their optical transitions

2004 J. Phys.: Condens. Matter 16 7405

(http://iopscience.iop.org/0953-8984/16/41/020)

INSTITUTE OF PHYSICS PUBLISHING JOURNAL OF PHYSICS: CONDENSED MATTER

J. Phys.: Condens. Matter **16** (2004) 7405–7417 PII: S0953-8984(04)84392-3

Determining the possible lattice sites of two unknown defects in orthoclase from the polarization effects in their optical transitions

M A Short

Department of Physics, Simon Fraser University, Burnaby, BC, Canada

E-mail: mashort@sfu.ca

Received 30 July 2004, in final form 21 September 2004
Published 1 October 2004
Online at stacks.iop.org/JPhysCM/16/7405
doi:10.1088/0953-8984/16/41/020

Abstract

The intensity of the optically excited 3.1 eV emission from an irradiated feldspar depends on the polarization of the 1.45 eV exciting light, and the 3.1 eV emission is itself polarized. Dipolar transitions are shown to account for the data in both cases. A method is proposed for using the dipole directions deduced from the data to determine the possible lattice sites of the defects in which these optical transitions occur. The method works by assuming the dipole direction will coincide with a symmetry direction of the crystal field around the defect and then checking the crystal structure for sites where this symmetry direction occurs. Two pairs of dipole directions were deduced from the data for both the excitation and the emission, and the directions of one pair aligned close to approximate symmetry axes in the average geometry of the four oxygen anions around the two T1 sites. It is concluded that transitions in defects occupying T1 sites are the most likely explanation for both the excitation and the emission.

1. Introduction

When some irradiated natural feldspars are optically excited they emit photons with energies which are greater than those of the excitation and this phenomenon is used for optical dating (see e.g. Aitken 1998). The mechanism is not fully understood, but the emission is believed to result from excitation of electrons trapped at defects after the irradiation. The basic idea is that electrons are optically excited to some higher state of the trap, from where they escape and subsequently recombine with holes trapped on other defects—some emitting a photon in the process. A full understanding of the physics of the luminescence process requires knowledge about the types of defects where the optical transitions are taking place, and where in the lattice these defects sit. The excitation and emission spectra are usually comprised of more than one broad band indicating that transitions in more than one type of defect may be involved (see

e.g. Baril and Huntley 2003). A few of these bands have been convincingly associated with particular defects, on the basis of defect abundance, optical excitation spectra, and theoretical calculations, but for many, including the important 1.45 eV (850 nm) resonance excitation and the 3.1 eV (400 nm) emission bands, the associations proposed so far are highly speculative (see e.g. Bailiff and Poolton 1991, Krbetschek *et al* 1997).

The difficulty in identifying the defects involved in the luminescence process is due to a number of factors. First, only a relatively small number of defects (as low as 100 ppm) are required for there to be significant luminescence, and these may be difficult to detect (Telfer and Walker 1975). Second, when charge recombines with an impurity element, whether it luminesces or not depends on its valence state which is not determined by methods used to quantify the abundance of an impurity element. Furthermore, natural samples may have inclusions rich in particular elements but these inclusions play no part in the luminescence process. Last, there are usually many different types of defects present in a sample and these can interact with each other to quench or sensitize the emission (Marfunin 1979, p 160), making it difficult to identify the luminescence centres based on the abundance of one type of defect.

What is reported on here is a proposed method for determining the lattice sites of the unknown defects from the polarization dependence of the optical transitions within the defect. This information will reduce the number of potential defects that can account for the observed optical transitions.

2. Theory

A preliminary account of the present work was given by Short and Huntley (2000). They measured the 1.45 eV photon-excited, 3.1 eV emission from three thin slices ($\approx$0.5 mm) of an orthoclase feldspar crystal (their reference No K3). The three slices were approximately orthogonal to each other so that two of the three principal directions, with refractive indices of n_x, n_y or n_z, were lying approximately in the plane of each slice. The emission intensity was found to depend on the polarization direction of the exciting photons, and the emission was itself polarized. Birefringence affects the polarization of a photon as it travels through a crystal, and a simple model was used to relate observations to atomic emissions or absorptions. The two main assumptions of the model were that both the excitation and the emission processes were dipolar, and that the dipole direction associated with a transition in one defect was the same for all defects of the same type.

In figure 1 a diagram is shown of the coordinate system used to calculate the effect of the birefringence on linearly polarized photons as they travel parallel to the z direction. The projection of the dipoles onto the plane normal to the z direction makes an angle φ with one of the principal directions lying in that plane. The angle θ is the direction of the transmission axis of an external polarizer used to analyse the emission or polarize the excitation.

An expression for the emission intensity I was derived from the model by calculating the effect on photons travelling to or from one thin layer, then integrating over the thickness of the crystal i.e.

$$I \propto \cos^2(\varphi)\cos^2(\theta) + \sin^2(\varphi)\sin^2(\theta) + \frac{2\cos(\varphi)\sin(\varphi)\cos(\theta)\sin(\theta)}{kd}\sin(kd) \qquad (1)$$

where k is a variable dependent on the photon energy and on the difference in the refractive indices of the two principal directions lying in the plane (n_x–n_y). Equation (1) predicts that the intensity is a maximum when the transmission axis of the external linear polarizer is parallel to a principal direction of the crystal. Note that equation (1) only applies for sample slices cut so that two of the principal directions lie in the plane (which automatically means the third

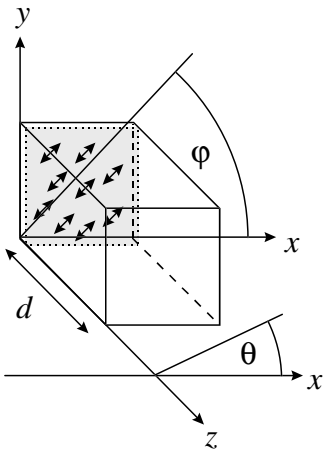

Figure 1. System of axes and angles used to account for birefringence effects on the polarization of light travelling in the z direction of a crystal of thickness d. The shaded plane is a thin layer normal to the z direction, and the black arrows represent dipoles within the layer for either the emission or excitation centres.

principal direction is normal to the plane). Furthermore, the same equation applies to both linearly polarized excitation and linearly polarized emission. However, the equation does not allow for a reduction in the excitation or emission intensity due to absorption, and thus will only apply to nearly transparent samples.

For $d \geqslant 0.5$ mm the first two terms in equation (1) are predominant (the third term contributing a few per cent at most to the variation in emission) and these two terms were shown to fit the data obtained by Short and Huntley (2000) very well. The φ values obtained from the fits were found to be consistent with two pairs[1] of dipole directions for both the excitation and the emission.

Dipolar transitions should be expected in a crystal defect. Simple crystal field theory predicts that they will occur for some transitions if the defect is subjected to a non-cubic crystal field (see e.g. Cotton 1990, p 296). Furthermore, the dipole associated with a dipolar transition will align with a symmetry axis of the field which will be predominantly due to its nearest neighbours. In the more advanced ligand field and molecular orbital theories, the interaction between the electronic wavefunctions of the defect and its nearest neighbours is taken into account; nevertheless, dipolar transitions can still occur between the hybridized wavefunctions of the defect, and the associated dipole will align with a symmetry axis in the geometry of its nearest neighbours (see e.g. Cotton 1990, p 254).

In a real crystal there will be a large number of identical defects occupying equivalent lattice sites distributed over its whole volume, and thus the average polarization effect will be a sum of all the dipolar transitions of all the defects. If the crystal symmetry results in non-parallel dipole directions for the individual dipolar transitions, then the polarization effect will be smeared out. The worst case of smearing would occur for a crystal where the defects are in two equivalent sites, but these sites result in perpendicular dipole directions, in which case there will be no observed polarization effect. Such a situation would exist for a crystal with cubic symmetry. The superposition of different polarizations due to other crystal symmetries

[1] Since φ values can be both positive or negative this leads to two pairs of possible dipole directions where one of each pair is a mirror image of the other reflected through the (0 1 0) plane. Any one of the four dipole directions can account for the data. Short and Huntley (2000) gave directions for one of each pair.

would have to be calculated on a case by case basis. It is shown in the appendix that dipolar transitions at equivalent lattice sites in orthoclase would not result in a smearing out of the polarization effect. Thus, in this case the first two terms of equation (1) are still applicable for determining what the possible dipole directions are from the polarization data.

Apart from the main assumptions used in the model, two experimental conditions were considered important by Short and Huntley (2000) in order for equation (1) to be correctly applied: one involving orientation of the principal directions to the sample slices has already been mentioned; the other requires both the exciting photons at the sample and the measured emission to be well collimated. These conditions were approximately fulfilled in the original work, but there was room for improvement. Thus the original experiment was repeated using an apparatus with better light collimation, and slices of an orthoclase crystal that were all cut so that the approximation of two principal directions lying in a plane was more accurate. Clear polarization effects were measured, similar to those found in the earlier work. Two pairs of dipole directions were deduced from both the excitation and emission data, and in each case one pair was found to align closely with symmetry directions in the geometry of the nearest neighbours to the T1 sites in orthoclase. Thus it is concluded that transitions in defects at T1 sites are the most likely explanation for both the 1.45 eV excitation and 3.1 eV emission.

3. Experimental details

Only a brief description of the sample and the experimental set-up is given here; further details are in the original work and in Short (2003). For consistency with previous results, the orthoclase feldspar K3 was again chosen for these new polarization measurements. The sample was made up of many transparent single crystals ranging from a few millimetres to a few centimetres on their longest side. The sample composition was 12% potassium, 2.22% sodium, and 0.04% calcium (Huntley *et al* 1988), and various trace elements (Short 2003). There were no obvious signs of crystal twinning. Slices $\approx$0.5 mm thick and $\approx$1 mm^2 were cut from larger crystals so that the two largest surfaces of each slice were parallel to (0 0 1), (3 0 $\bar{1}$), and (0 1 0). These slices were called A, D′, and E respectively. The slices were polished using 600 grade carborundum paper, and then 1.0 μm polishing powder. Light transmission experiments were conducted on the samples (Short 2003) which indicated that there was no significant absorption in the range from 1.45 to 3.3 eV (380–850 nm).

The principal directions of the refractive index were determined for each sample slice by optical microscopy, and two were found to be lying in the plane of each slice (with an estimated error of a few degrees), consistent with the diagram given by Deer *et al* (1992, figure 144). Each slice was given a gamma dose[2] of about 1.0 kGy and then placed, with one of its large surfaces down, into silicone oil on glass slides and pressed down to ensure good contact. The glass slides themselves were not irradiated to avoid any spurious luminescence effects from the glass. One set of sample slices was preheated at 110 °C for 12 h after the irradiation, and another set was left unpreheated.

Optical excitation of the samples was by a well collimated (solid angle $\approx 10^{-3}$ sr) beam of 1.45 eV photons (see figure 2) from a single light emitting diode (LED)[3]. To control the excitation, an electronic shutter was placed between the LED and the sample. Polarized exciting light was obtained by placing an Oriel[4] dichroic polarizer (P1), type 27361, in the

[2] The irradiation, subsequent storage, and preheatings were all carried out in the dark. The mounting of the samples was carried out in dim orange light.

[3] Short and Huntley (2000) used a circular array of LEDs; this was changed here to a single LED to improve the collimation of the exciting light.

[4] Oriel Instruments, 150 Long Beach Boulevard, Stratford, CT 06615-0872, USA.

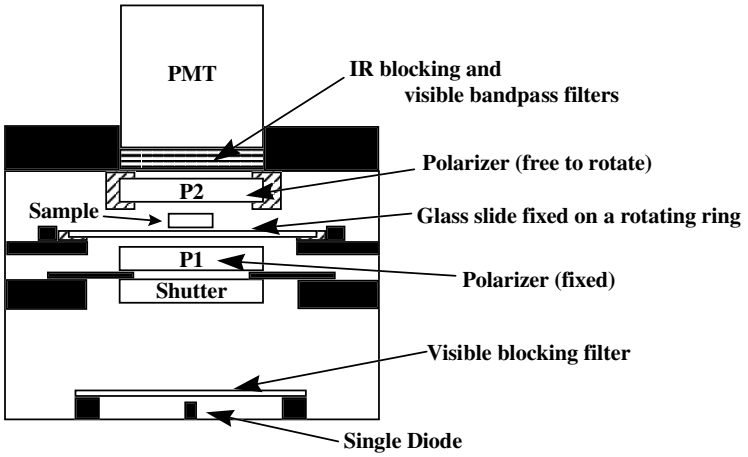

Figure 2. Schematic diagram of the equipment used to measure changes in the emission intensity from thin sample slices (not to scale). The visible-blocking filter placed over the LED was used to block any visible emissions it may have.

light path before the sample. The polarizer was held in a fixed position and could not rotate. A glass slide, on which a sample slice was mounted, was placed on a rotating ring so that the sample was centred directly over the LED. A scale was marked on the circumference of the rotating ring, so the angular position (ζ) of an arbitrary mark on the sample slide relative to the polarizer transmission axis could be measured. After completion of a measurement the relation between the mark on the slide and a principal direction of the sample slice was determined. The power of the polarized exciting light per unit area at the sample slice was about 250 μW cm^{-2}.

Emission was detected by an EMI[5] 9635QB (blue sensitive) photomultiplier tube (PMT), and photon counting electronics. Glass filters, a Kopp[6] 5-58 and a Schott[7] BG 39 (3 mm thick), were placed in front of the PMT photocathode so that only luminescence from the 3.1 eV emission band was measured, and scattered 1.45 eV excitation photons were not. Since there was a need to collect sufficient photon counts for good statistics without reducing the luminescence intensity too much, the solid angle between the sample slice and the PMT photocathode had to be large. The PMT aperture diameter was 38 mm, and measurements were made with two PMT to sample slice distances of 70 and 110 mm. Using these values, emission was measured with solid angles of 0.23 and 0.1 sr respectively. Although the latter was an improvement on the original equipment used by Short and Huntley (2000, 0.4 sr), the emission was not as well collimated as the excitation, but measurements at the two different solid angles should show how sensitive the results were to the collimation. For analysing the polarization of the emission, a second Oriel dichroic polarizer (P2), type 27341, was placed in the light path between a sample slice and the PMT.

The procedure for measuring how the 3.1 eV emission intensity changed with the polarization direction of the excitation was to first measure the intensity from a sample slice over a 2 s excitation. There was no second polarizer (P2) between the sample slice and the PMT as shown in figure 2. The sample slice was then rotated 10° and exposed to the excitation for another 2 s. This was repeated 17 more times, for a total rotation of 180°. A background

[5] Electron Tubes Inc., 100 Forge Way, Unit F, Rockaway, NJ 1923, USA.
[6] Kopp Glass Inc., 2108 Palmer Street, Pittsburgh, PA 15218, USA.
[7] Schott Glass Technologies Inc., 400 York Avenue, Duryea, PA 18642, USA.

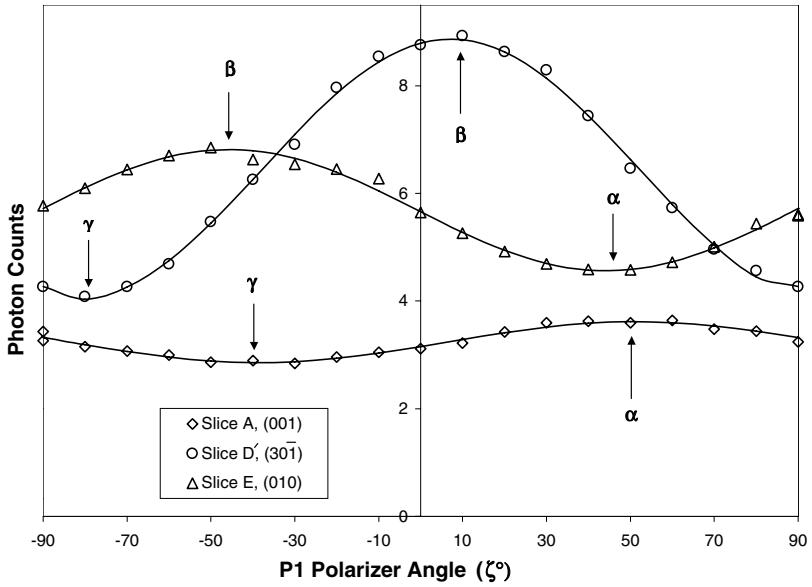

Figure 3. Changes in the emission intensity as a function of the polarization direction of the excitation for irradiated, but unpreheated, slices of K3. α, β, and γ are the principal directions. The solid curves are fits to the data using the first two terms of equation (1). Uncertainties due to photon counting statistics are contained within the symbols. Repeat measurements (not shown) on a set of sample slices that were preheated after the irradiation revealed emission with the same ζ dependence, but at about half the intensity.

count (around 50 counts s^{-1}) was obtained by repeating the measurements using unirradiated samples slices, and this was subtracted from the number of photon counts. The emission intensity of a sample decreased by about 3% as a result of the 19 measurements; the precise reduction depended on which sample slice was measured. The intensities were corrected for this reduction by assuming the reduction was a constant percentage for each 2 s measurement. The corrected data were then plotted against ζ. A similar procedure was used for analysing the polarization of the emission except that in this case the glass slide was held fixed and the polarizer P2 rotated.

4. Results

The intensity of the 3.1 eV emission clearly depended on the polarization of the 1.45 eV exciting photons (figure 3), with maxima and minima occurring when the transmission axis of the polarizer was parallel (within experimental error) to principal directions that lie in the plane of each sample slice. The 3.1 eV emission was itself polarized (figure 4), with an angular dependence that did not depend on the polarization of the 1.45 eV exciting photons, nor on the different sample to PMT distances. Table 1 gives a summary of the polarization results.

5. Dipole directions and the crystal structure

Two pairs of dipole directions were deduced from the $\pm\varphi$ angles for the 1.45 eV excitation given in table 1: [$\bar{4}4$ 46 100] and [$\bar{4}4$ $4\bar{6}$ 100], and [82 25 100] and [82 $2\bar{5}$ 100]. Two similar pairs of dipole directions were deduced from the $\pm\varphi$ angles for the 3.1 eV emission:

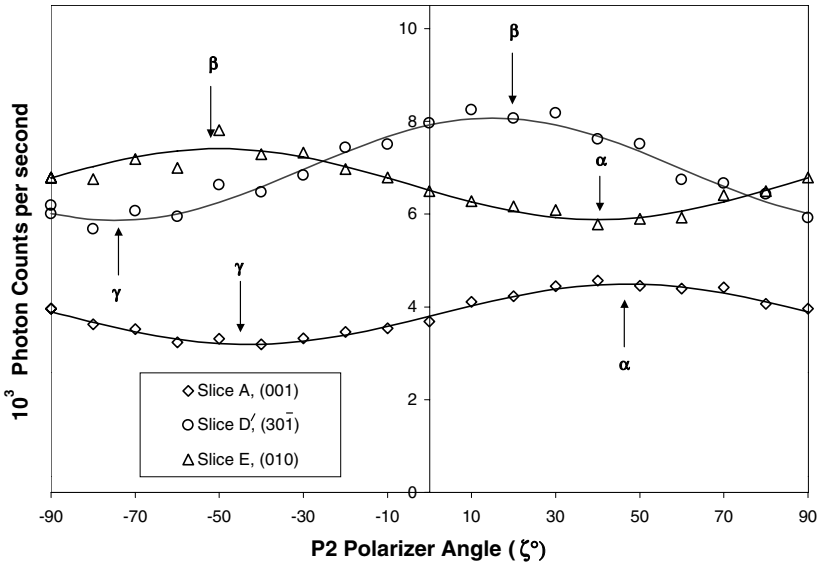

Figure 4. Changes in the emission intensity as a function of the polarization direction of the emission for irradiated, but unpreheated, slices of K3. α, β, and γ are the principal directions. The solid curves are fits to the data using the first two terms of equation (1). Uncertainties due to photon counting statistics are contained within the symbols. Repeat measurements (not shown) on a set of sample slices that were preheated after the irradiation revealed emission with the same ζ dependence, but at about half the intensity.

Table 1. The three headings identify the sample slice and the direction in which the emission or excitation was propagating. The entries for each slice indicate the polarization direction for maximum and minimum emission and the $\pm\varphi$ angles obtained from fits to the data using the first two terms of equation (1).

Summary of polarization results from K3									
	Slice A (0 0 1), β[a]			Slice D′ (3 0 $\bar{1}$), α			Slice E (0 1 0), γ		
	α[a]	γ[a]	$\pm\varphi$ (deg)	β	γ	$\pm\varphi$ (deg)	α	β	$\pm\varphi$ (deg)
1.45 eV excitation	Max	Min	41	Max	Min	34	Min	Max	39
3.1 eV emission	Max	Min	40	Max	Min	40	Min	Max	42

[a] For slice A the propagation and polarization directions were not aligned precisely parallel with α, β, and γ, but were skewed about 8° from alignment (see Deer *et al* 1992, figure 144).

[5$\bar{3}$ 54 100] and [5$\bar{3}$ 5$\bar{4}$ 100], and [88 30 100] and [88 3$\bar{0}$ 100]. The uncertainties in these directions were estimated to be ≈3°. The dot products calculated between the dipole directions for the excitation and those for the emission shows the two sets of dipoles deviate by ⩽4.5°.

The above dipole directions and the average crystal structure of orthoclase were viewed together using a 3D plotting program, and one pair was found to align close to symmetry directions in the geometry of the four anions around the T1 sites. These alignments will be described for the dipoles deduced from the excitation data, but similar alignments occur for the dipoles deduced from the emission data. To aid understanding of these alignments, the T1 sites of orthoclase are described as either $T1_o$ or $T1_m$ as in microcline feldspar. In microcline the distinction between these two site types is necessary because the sites are not related by symmetry, but for orthoclase this is an artificial distinction, because these T1 sites are related

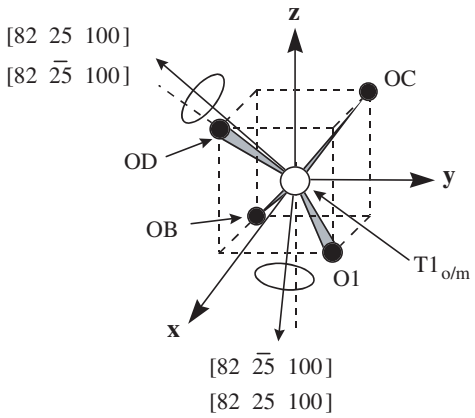

Figure 5. Sketch showing the alignment of the dipoles deduced from data to the T1 sites. The way to interpret this figure is as follows. When the cation occupies the $T1_o$ site of the feldspar lattice, then the [82 25 100] dipole points close to the direction from the cation to its OD anion, and the [82 $\bar{2}$5 100] dipole points close to a line from the cation which bisects the angle between its O1 and OB anions (the $-z$ direction in the figure). The ellipses shown in the sketch represent the experimental error (exaggerated for clarity) in the direction of the dipoles. When the cation occupies the $T1_m$ site of the feldspar lattice, then the [82 $\bar{2}$5 100] dipole points close to the direction from the cation to its OD anion, and the [82 25 100] dipole now points close to a line from the cation which bisects the angle between its O1 and OB anions.

by $C2/m$ symmetry[8]. The distinction is introduced here because there is an ambiguity in assigning dipole directions to symmetry directions around T1 sites. This problem arises as follows—if the four possible dipoles are compared in turn with the crystal structure, one of one pair (call it No 1) is found to align well with a symmetry axis of a T1 site (call it $T1_o$). The other dipole direction (No 2) of the pair is then found to align with the same symmetry axis of a mirror image of the $T1_o$ site ($T1_m$) as it should with a $C2/m$ symmetry group. However, if one continues comparing the dipoles with the structure it is also found that No 1 dipole direction aligns with a different symmetry direction of the $T1_m$ site and No 2 dipole direction aligns with the same symmetry direction of $T1_o$ site. The latter is not a general property of $C2/m$ groups, but is merely a coincidence that comes about because the T1 $\rightarrow$ OC bond direction in orthoclase (see figure 5) is approximately parallel to the [0 1 0] axis. Thus a π rotation about this axis (equivalent to switching the symmetry directions of the four anions between those of $T1_o$ and $T1_m$) causes two different symmetry directions to approximately align with the same dipole direction. Thus it is not possible to unambiguously assign dipole directions to one particular symmetry direction—there are two possibilities.

The [82 25 100] dipole was aligned approximately along the direction from a $T1_o$ cation to its OD anion (figure 5). Since the anions are arranged at the vertices of an approximately regular tetrahedron, this direction is an approximate threefold symmetry axis. This same dipole also lies approximately in the plane made by a $T1_m$ cation and two of its anions (OB and O1) and bisects the angle made between the bonds. The latter is an approximate twofold symmetry axis. Just how close this dipole direction is to these crystal directions can be seen by taking the dot product of the vector for the dipole with the vector for a direction in the crystal. The results are listed in table 2.

[8] In microcline the $T1_o$ and $T1_m$ sites contain predominantly Al and Si ions respectively, causing the structure to become triclinic. In orthoclase the Al and Si ions are in roughly equally proportions in both T1 sites, maintaining an average monoclinic structure.

Table 2. This table shows how close the dipole directions are to certain directions in orthoclase by calculating the dot products between them. The first column contains the dipole directions deduced from the polarization data. The headings of the next four columns are the vectors, calculated from x-ray diffraction data (Colville and Ribbe 1968), for particular directions in the crystal. The $(OB + O1)_i$ notation refers to the direction from the $T1_i$ cation that bisects the angle between its OB and O1 anion bonds. The assignment of the sites as either 'o' or 'm' is arbitrary; interchanging the 'o' or 'm' indices does not affect the angles.

The angles between the deduced dipoles and certain crystal directions				
Dipole directions	Crystal directions			
	$T1_o \rightarrow OD_o$	$T1_m \rightarrow OD_m$	$T1_m \rightarrow (OB + O1)_m$	$T1_o \rightarrow (OB + O1)_o$
1.45 eV excitation	[94 32 100]	[94 $\bar{3}2$ 100]	[87 34 100]	[87 $\bar{3}4$ 100]
[82 25 100]	7.0°	—	6.4°	—
[82 $\bar{2}5$ 100]	—	7.0°	—	6.4°
3.1 eV emission	[94 32 100]	[94 $\bar{3}2$ 100]	[87 34 100]	[87 $\bar{3}4$ 100]
[88 30 100]	2.9°	—	2.6°	—
[88 $\bar{3}0$ 100]	—	2.9°	—	2.6°

The [82 $\bar{2}5$ 100] dipole is similar to the [82 25 100] dipole except that it is reflected through the (0 1 0) plane. This reflection means that the dipole aligns with the crystal structure in a similar way as the [82 25 100] dipole, except there is an interchange in the 'o' and 'm' indices of the T1 cations that it aligns with, i.e. it is aligned approximately along the direction from a $T1_m$ cation to its OD anion, and along the line from a $T1_o$ cation that bisects the angle between the bonds of its OB and O1 anions.

The [$\bar{4}4$ 46 100] and [$\bar{4}4$ $\bar{4}6$ 100] dipole directions did not appear to align close to any approximate symmetry directions of any sites in the orthoclase structure. Since the dipoles deduced from the emission data were similar to those deduced from the excitation data they align with the same crystallographic directions as indicated by the size of angle of deviation given in table 2.

6. Discussion

Electronic transitions in various defects in various host crystals have been observed to occur with the absorption and emission of photons with a preferred polarization (e.g. Sayre *et al* 1955, Feofilov 1961, Piper and Carlin 1961, Runciman *et al* 1973a, 1973b, Goldman and Rossman 1977, Hofmeister and Rossman 1983, 1984, White *et al* 1986, Cotton 1990). Transitions can be electric or magnetic dipole, or electric quadrupole. Electric dipole transitions have the most probability of occurring, by several orders of magnitude, and are thus the most common transition observed, leading to the emission or absorption of either linearly or circularly polarized light (Cotton 1990). The exact nature of the polarization depends on the type of transition and on the symmetry in the geometry of the nearest neighbours to the defect. To obtain a dipolar transition, the geometry of nearest neighbours must have axial symmetry, and the associated dipole will be parallel to this axis. In simple cases where the symmetry axes in the nearest neighbour geometry around equivalent defects all point in the same direction, good agreement can be obtained between the expected polarization effect in the absorption of light by the defects and the experimental results (e.g. Piper and Carlin 1961). In more complicated cases considerable effort is required to understand the distribution of defects and the geometry of the nearest neighbours to them before one can explain the observed polarization effect (e.g. Goldman and Rossman 1977).

The results of the experiments described here clearly show that emission intensity depended on the polarization of the excitation, and that the emission was itself polarized. The most likely explanation is transitions in defects which are surrounded by nearest neighbours in a geometry with non-cubic symmetry. The data shown in figures 3 and 4 were in good agreement with the earlier work, as was the fact that the polarization effect did not change for preheated and unpreheated samples. The simplest model one can think of that would explain this is two or more similar types of 1.45 eV excitable trap that occupy the same sites throughout the lattice, and electrons trapped there have different thermal lifetimes. The latter may occur because the traps have slightly different local environments, but with the same site symmetry which results in the same polarization effect. Another possibility is that the local environments around all the 1.45 eV excitable traps are identical, thus the polarization effect is constant, but the trapped electrons tunnel to the recombination centres after thermal excitation and thus the thermal lifetimes of the trapped electrons depend on the proximity of the recombination centres.

One of each pair of dipoles deduced from the data were similar to the ones found by Short and Huntley (2000, [3 1 3] and [$\bar{1}$ $\bar{1}$ 3]); the slight differences in directions may be due to the better light collimation used here and to the fact that all the sample slices were cut so that the approximation of two principal directions lying in the plane was more accurate. Also consistent with the earlier results was the fact that the sets of dipole directions deduced from the excitation and emission data were very similar. However, it is clear from figures 3 and 4 that the polarization effect is significantly different for excitation and emission especially for slice D′. The reason for this apparent dichotomy is because equation (1) is quite sensitive to changes of φ, and thus significantly different polarization effects can be caused by dipoles which have similar directions.

To summarize, one pair of dipole directions deduced from the excitation data, and one pair deduced from the emission data, aligned close to the same approximate symmetry directions in the geometry of the T1 sites and their four anions (table 2). This would be consistent with both the excitation and the emission transitions taking place in defects that occupy T1 sites that have an axial symmetry in one of the two possible directions found, but the data are insufficient for determining which one. Although the average crystal geometry shows the T1 sites only have approximate axial symmetry axes in either of the two dipole directions, it is reasonable to postulate that such a symmetry axis exists around a T1 site occupied by a defect. Two possible distortions of a regular tetrahedron would lead to a geometry with a single symmetry axis; in both cases the angles between bonds remain similar to that of a regular tetrahedron. In one case the T1 → OD anion bond is a different length from the other bonds; in the other case the anion bond lengths group into two pairs (T1 → OB and T1 → O1) and (T1 → OC and T1 → OD) of different lengths. In the first case one would have a threefold symmetry axis parallel to the T1 → OD bond and in the second case a twofold symmetry axis parallel to the z axis (figure 5).

In orthoclase the Al^{3+} ions primarily occupy T1 sites. A host of other ions may substitute for the Al^{3+} ions and thus these will also be found predominantly in T1 sites. The only two feldspar defects that have been suggested for emission close to 3.1 eV are Cu^{2+} and Eu^{2+} impurities (Krbetschek *et al* 1997); however, neither of these are found in T1 sites, and therefore they must be rejected. No alternative defects can be proposed at this time to account for the polarized 3.1 eV emission. The only suggestions found in the literature for defects accounting for the 1.45 eV excitation resonance are hole centres (Bailiff and Poolton 1991) which are created when ionizing radiation removes an electron from a normal oxygen anion changing its valence from O^{-2} to O^{-1}. Speit and Lehmann (1976,1982), and Hofmeister and Rossman (1985) found a correlation between an optical absorption band peaked at around 1.45 eV and

an EPR signal for a hole centre. However Speit and Lehmann also showed that the EPR signal disappears at room temperature, but can be recovered by cooling the sample back to 77 K. The latter indicates that the hole centres are not localized at particular oxygen sites at room temperature. Since there are five non-equivalent oxygen anions in feldspar, and a hole centre can occupy any one at room temperature, the polarization effect of a postulated 1.45 eV optical transition would be smeared out. Thus the proposed hole centre is not a viable candidate. A possibility that may explain both EPR data and polarization data is that electrons are trapped at defects in T1 sites after irradiation simultaneously with the creation of hole centres.

7. Conclusion

The 3.1 eV emission intensity clearly depended on the polarization of the 1.45 eV exciting photons and the 3.1 eV emission was itself clearly polarized. Dipoles deduced from the data closely aligned with approximate symmetry directions in the crystal structure of the T1 sites, indicating that transitions in defects at these sites may be responsible for the excitation and the emission. None of the defects that have been previously suggested for the excitation and the emission occupy T1 sites and thus they are rejected. Although equation (1) only applies to nearly transparent crystals it is relatively straightforward to introduce terms that take into account a uniform absorption of photons as they propagate through the sample (Short 2003). This opens up the possibility of applying the method to a wider range of samples. However the theory with, or without, taking absorption into account requires a number of assumptions and approximations—and it is not clear if these are all completely justified. Therefore, at this stage, one cannot rule out the possibility that the alignments that were found for K3 are merely coincidental. One way to test the method is to apply it to optical transitions in known defects occupying known lattice sites. This was done for Fe^{3+} ions that are known to occupy T1 sites in feldspars and it was found that the same methods as used here correctly predicted the location of the defects. Furthermore, the symmetry axes of the nearest neighbours around the Fe^{3+} ions deduced from the polarization data were found to be consistent with EPR data, and group theory calculations predicting the polarization effect of different transitions were consistent with those observed.

Acknowledgments

I would like to thank L Groat for providing me with the K3 orthoclase sample and D J Huntley for assistance with the preparation of this manuscript. This research was supported by a grant from the Natural Sciences and Engineering Research Council of Canada to DJH.

Appendix

Orthoclase has a monoclinic structure with twofold rotational symmetry about the [0 1 0] axis and mirror symmetry through the (0 1 0) plane. If any general vector $[u\ v\ w]$ is rotated about the [0 1 0] axis by π it becomes $[\bar{u}\ v\ \bar{w}]$; or if it is reflected through the (0 1 0) plane it becomes $[u\ \bar{v}\ w]$ (see figure A.1). A double operation on the $[u\ v\ w]$ vector of a π rotation and a reflection through the (0 1 0) plane transforms it to $[\bar{u}\ \bar{v}\ \bar{w}]$. However, $[\bar{u}\ \bar{v}\ \bar{w}]$ is parallel to $[u\ v\ w]$, and $[\bar{u}\ v\ \bar{w}]$ is parallel to $[u\ \bar{v}\ w]$. Therefore, one can conclude that any $[u\ v\ w]$ vector associated with a particular site in orthoclase occurs for all equivalent sites throughout the crystal as either parallel to $[u\ v\ w]$ or parallel to $[u\ \bar{v}\ w]$. When the crystal is viewed in an arbitrary direction then the two vectors $[u\ v\ w]$ and $[u\ \bar{v}\ w]$ appear to have lengths ℓ_1 and

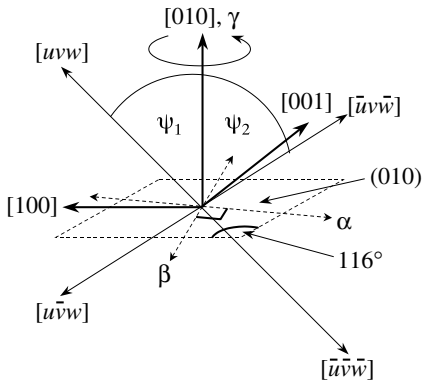

Figure A.1. Sketch showing how an arbitrary vector [u v w] in a monoclinic coordinate system transforms with a π rotation about the [0 1 0] axis or a reflection through the (0 1 0) plane. The [1 0 0] axis lies in the plane of the page of this sketch, but the [0 1 0] axis does not. α, β, and γ are principal directions. The γ axis is parallel to the [0 1 0] axis, and the α and β axes lie in the (0 1 0) plane but are not parallel with either the [1 0 0] or [0 0 1] axes. The angles ψ_1 and ψ_2 are the angles that the vectors [u v w] and [$\bar{u}$ v $\bar{w}$] appear to make with the projection of the [0 1 0] axis in the plane. In this oblique view it appears that $\psi_1 \neq -\psi_2$, and the vector lengths appear not to be the same, but there would be equality if the view were normal to the [0 1 0] axis.

ℓ_2, and appear to make angles ψ_1 and ψ_2 with the projection of the [0 1 0] axis in the plane normal to the viewing direction. However, when the view is normal to the [0 1 0] axis then $\ell_1 = \ell_2$ and $\psi_1 = -\psi_2$, whereas if the crystal is viewed parallel to the [0 1 0] axis then the two vectors appear to be the same length and parallel.

A dipole associated with a dipolar emission or excitation transition in a defect that occupies equivalent sites in orthoclase will have the same vector properties as described above. The emission intensity will be proportional to the square of the apparent length of the dipole in a plane normal to the viewing direction. The birefringence will affect the polarization of photons as they travel through the crystal to or from a dipole as described earlier. Equation (1) describes the effect, assuming a uniform distribution of dipoles all pointing in the same direction, and only applies for sample slices cut so that two of the principal directions lie in the plane. Now contributions from two different dipole directions must be considered. However, since γ is parallel to [0 1 0], the two slices that contain the γ axis and either α or β will have $\ell_1 = \ell_2$ and $\psi_1 = -\psi_2$ for the two dipoles. In this case the first two terms of equation (1) are still applicable, and the $\pm\varphi$ parameters obtained from a fit to the data are equal to ψ_1 and ψ_2.[9] The viewing direction of a slice of the crystal cut so that α and β lie in the plane is parallel to the [0 1 0] axis, thus the two dipoles will appear in this view to be the same length and parallel. In this case the fitting of the first two terms of equation (1) to the data will result in $\pm\varphi$ parameters, one of which will be the angle the projection of the dipoles make with one of the principal directions in the (0 1 0) plane.

References

Aitken M J 1998 *An Introduction to Optical Dating* (Oxford: Oxford University Press)
Bailiff I K and Poolton N R J 1991 Studies of charge transfer mechanisms in feldspars *Radiat. Meas.* **18** 111–8

[9] This can be seen by taking a sum of two equations (1) where $\ell_1 = \ell_2$ and $\psi_1 = -\psi_2$; the result is the cancellation of the third terms.

Baril M R and Huntley D J 2003 Infrared stimulated luminescence and phosphorescence spectra of irradiated feldspars *J. Phys.: Condens. Matter* **15** 8029–48

Colville A A and Ribbe P H 1968 The crystal structure of an adularia and a refinement of the structure of orthoclase *Am. Mineral.* **53** 25–37

Cotton F A 1990 *Chemical Application of Group Theory* 3rd edn (New York: Wiley)

Deer W A, Howie R A and Zussman J 1992 *An Introduction to the Rock Forming Minerals* 2nd edn (England: Longman)

Feofilov P P 1961 *The Physical Basis of Polarized Emission* (New York: Consultants Bureau)

Goldman D S and Rossman G R 1977 The spectra of iron in orthopyroxene revisited: the splitting of the ground state *Am. Mineral.* **62** 151–7

Hofmeister A M and Rossman G R 1983 Color in feldspar *Feldspar Mineralogy* (*Reviews in Mineralogy* vol 2) ed P H Ribbe (Washington: Mineral Society of America)

Hofmeister A M and Rossman G R 1984 Determination of Fe^{3+} and Fe^{2+} concentrations in feldspar by optical absorption and EPR spectroscopy *Phys. Chem. Miner.* **11** 213–24

Hofmeister A M and Rossman G R 1985 A model for irradiative coloration of smoky feldspar and the inhibiting influence of water *Phys. Chem. Miner.* **12** 324–32

Huntley D J, Godfrey-Smith D I, Thewalt M L W and Berger G W 1988 Thermoluminescence spectra of some minerals relevant to thermoluminescence dating *J. Lumin.* **39** 123–36

Krbetschek M R, Götze J, Dietrich A and Trautmann T 1997 Spectral information from minerals relevant for luminescence dating *Radiat. Meas.* **27** 695–748

Marfunin A S 1979 *Spectroscopy, Luminescence and Radiation Centers in Minerals* (Berlin: Springer)

Piper T S and Carlin R L 1961 Polarized visible spectra of crystalline trisoxalatometallates *J. Chem. Phys.* **35** 1809–14

Runciman W A, Sengupta D and Gourley J T 1973a The polarized spectra of iron in silicates. II. Olivine *Am. Mineral.* **58** 451–6

Runciman W A, Sengupta D and Marshall M 1973b The polarized spectra of iron in silicates. I. Enstatite *Am. Mineral.* **58** 444–50

Sayre E V, Sancier K M and Freed S 1955 Absorption and quantum states of the praseodymium ion. I. Single crystals of praseodymium chloride *J. Chem. Phys.* **23** 2060–5

Short M A 2003 An investigation into the physics of the infrared excited luminescence of irradiated feldspars *PhD Thesis* Simon Fraser University, Burnaby, BC, Canada, unpublished

Short M A and Huntley D J 2000 Crystal anisotropy effects in optically stimulated luminescence of a K-feldspar *Radiat. Meas.* **32** 865–71

Speit B and Lehmann G 1976 Hole centers in the feldspar sanidine *Phys. Status Solidi* a **36** 471–81

Speit B and Lehmann G 1982 Radiation defects in feldspars *Phys. Chem. Miner.* **8** 77–82

Telfer D J and Walker G 1975 Optical detection of Fe^{3+} in lunar plagioclase *Nature* **258** 694–5

White W B, Matsumura M, Linnehan D G, Toshiharu F and Chandrasekhar B K 1986 Absorption and luminescence of Fe^{3+} in single-crystal orthoclase *Am. Mineral.* **71** 1415–9